

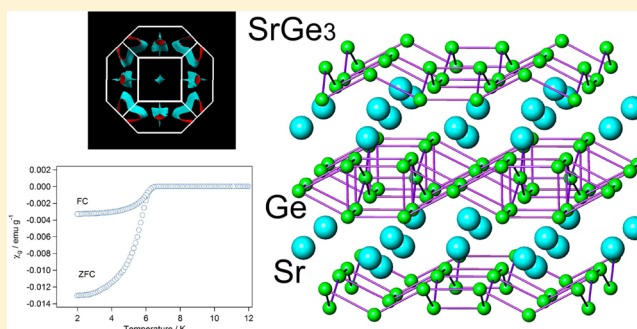
High-Pressure Synthesis and Electronic Structure of a New Superconducting Strontium Germanide (SrGe_3) Containing Ge_2 Dumbbells

Takuya Nishikawa, Hiroshi Fukuoka,* and Kei Inumaru

[†]Department of Applied Chemistry, Faculty of Engineering, Hiroshima University, Higashi-Hiroshima 739-8527, Japan

S Supporting Information

ABSTRACT: We obtained a new strontium germanide (SrGe_3) by high-pressure and high-temperature synthesis. It was prepared at 13 GPa and 1100 °C. The space group and cell constants are $I4/mmm$ (No. 139), $a = 7.7800(8)$ Å, $c = 12.0561(13)$ Å, and $V = 729.74(17)$ Å³. SrGe_3 crystallizes in the CaSi_3 structure composed of Ge–Ge dumbbells and Sr^{2+} ions. SrGe_3 is a type II superconductor with a transition temperature of 6.0 K.



INTRODUCTION

High-pressure and high-temperature synthesis is a promising technique to explore new compounds with new structures and interesting physical properties, especially for elements with a tendency to form covalent bonds. Germanides prepared by high-pressure synthesis show a variety of interesting structures, where germanium atoms form not only sp^3 -based structures but also structures composed of germanium atoms with an unusual coordination number induced by the high-pressure effect.^{1–10}

We have been investigating the reactions of germanium and electropositive elements at high pressure and have reported new germanides containing unusual coordinated germanium. In pentagermanide LaGe_5 ,^{1,2} which has a tunnel structure with lanthanum ions in the tunnels, one of the two independent germanium sites has a coordination number of 8. The site interconnects germanium layers formed by edge-sharing Ge_6 rings with a boat-type conformation. This germanide shows a superconducting transition at 6.8 K.

The two germanides LaGe_3 and BaGe_3 based on a mixed close-packed structure have been reported.^{3,4} Germanium atoms form regular triangle units in these germanides. In the case of BaGe_3 , the triangular units form Ge_6 elongated octahedra that stack to form one-dimensional columns (a B-site defected CsNiF_3 structure), whereas the triangles are isolated in the structure of LaGe_3 . These compounds are also superconductors with transition temperature $T_c = 4.0$ and 7.4 K for barium and lanthanum trigermanides, respectively. Recently, a new trigermanide (CaGe_3) has been reported. It contains Ge–Ge dumbbells and shows superconductivity with $T_c = 6.8$ K.⁵

In the present study, we investigated the reactions between strontium and germanium under high-pressure and high-

temperature conditions and obtained a new superconducting trigermanide. The electronic structure of the compound was investigated using full-potential density functional theory calculations.

EXPERIMENTAL SECTION

SrGe_3 was prepared by the following two-step reactions. A mixture of strontium (Aldrich, 99.9%) and germanium (Rare Metallic Co. Ltd., 99.999%) with a molar ratio of 1:2 was reacted in an argon-filled arc furnace to obtain SrGe_2 . The obtained SrGe_2 powder was mixed with germanium powder with a molar ratio of 1:1 SrGe_2/Ge (corresponding to $\text{Sr}:\text{Ge} = 1:3$) in an argon-filled box. The mixture was placed in a hexagonal boron nitride (h-BN) cell. The cell was placed in an octahedral MgO pressure medium with an edge size of 10 mm and heated at 13 GPa and 1100 °C using a Kawai-type multianvil press. The truncated edge length of the cubic anvil was 6 mm. After cooling to room temperature, the pressure was slowly released. A small bullet with a metallic luster was obtained.

Powder X-ray diffraction (XRD) measurements of the product were performed with a Bruker AXS D8 Advance diffractometer with nickel-filtered $\text{Cu K}\alpha$ radiation. The chemical composition of the product was analyzed by electron probe microanalysis (EPMA). The crystal structure of SrGe_3 was determined by single-crystal structure analysis. The diffraction intensity data were collected at room temperature for a single crystal with a size of $0.050 \times 0.050 \times 0.075$ mm³ on a Bruker Smart Apex II CCD diffractometer with graphite-monochromated $\text{Mo K}\alpha$ radiation. The structure was solved and refined using the Bruker SHELX software package.¹¹ Magnetic susceptibility measurements were performed on a polycrystalline sample with a SQUID magnetometer in a 20 Oe field.

The density of states (DOS) and band structure (k dispersion) of SrGe_3 were calculated by the Wien2k package with a full-potential

Received: May 6, 2015

Published: July 14, 2015



linearized augmented plane wave plus local orbitals code.^{12,13} The following parameters were used: muffin-tin radii (RMT) for strontium and germanium were 2.50 and 2.38, respectively; $RMT \times k_{\max} = 9$; number of k points = 10000; Perdew–Burke–Ernzerhof generalized gradient approximation. The software *XCrySDen* was used to draw the Fermi surfaces.¹⁴

RESULTS AND DISCUSSION

XRD suggested that the product contained a new germanide as the main phase. It also contained a small amount of $SrGe_{6-\delta}$, which is another strontium germanide formed only under high-pressure conditions.¹⁵ The XRD pattern is shown in Figure S1 in the SI. The diffraction pattern of the new phase was very similar to those of $CaGe_3$ and $CaSi_3$ with a tetragonal dumbbell structure.^{5,16} Chemical analysis by EPMA revealed that the new compound was a binary strontium germanide with a composition of $SrGe_{2.99}$.

We successfully prepared single crystals of $SrGe_3$ and performed single-crystal X-ray structure analysis. $SrGe_3$ crystallizes in space group $I4/mmm$ (No. 139) with a tetragonal unit cell with $a = 7.7800(8)$ Å, $c = 12.0561(13)$ Å, and $V = 729.74(17)$ Å³. The residual factors in the last least-squares refinement cycle converged on $R1 [I > 2\sigma(I)] = 1.10\%$ and $wR2$ (all) = 2.58%. The crystallographic data and details of the structure determination of $SrGe_3$ are listed in Table 1. The atomic and thermal displacement parameters are shown in Table 2.

Table 1. Crystallographic Data and Details on the Structure Determination of $SrGe_3$

| | |
|---|---------------------------------|
| formula | $SrGe_3$ |
| fw | 305.39 |
| space group | $I4/mmm$ (No. 139) |
| a (Å) | 7.7800(8) |
| c (Å) | 12.0561(13) |
| V (Å ³) | 729.74(17) |
| Z | 8 |
| cryst size (mm) | $0.05 \times 0.05 \times 0.075$ |
| diffractometer | Bruker APEX-II CCD |
| radiation (graphite-monochromated) | Mo $K\alpha$ |
| μ (Mo $K\alpha$) (mm ^{−1}) | 38.743 |
| 2θ limit (deg) | 54.84 |
| no. of obsd unique reflns | 280 |
| no. of variables | 16 |
| $R1, wR2 [I > 2\sigma(I)]$ | 0.0110, 0.0258 |
| $R1, wR2$ for all data | 0.0117, 0.0262 |
| goodness of fit, S | 1.173 |

The crystal structure of $SrGe_3$ is shown in Figure 1. The structure contains two groups of Ge–Ge bond distances with very different lengths. The shorter distances are 2.5325(9) Å for Ge1–Ge1 and 2.5432(7) Å for Ge2–Ge2, which are slightly

longer than the neutral covalent bond length of germanium in the diamond structure (2.45 Å). These bonds are considered Ge–Ge single bonds.

The longer Ge–Ge distances are 2.7811(3) and 2.8431(6) Å. Taking into account the longer distances, the whole structure of $SrGe_3$ is considered to be a layer structure, as shown in Figure 1a (Ge–Ge distances <2.85 Å are shown as purple sticks). The layer structure is composed of two-dimensional germanium layers and strontium ions, which are situated in the interlayer spaces, as shown in Figure 1a. Each germanium atom is five-coordinated.

Once the sticks for the longer distances are removed, the arrangement of Ge–Ge dumbbells can clearly be seen (Figure 1b). The chemical formula can therefore be described as $Sr_2(Ge_2)_3$. The dumbbells are parallel or vertical to neighboring dumbbells. Structures based on dumbbell units are popular in structural chemistry. Pyrite, which has S–S dumbbell units, is a famous example. Such dumbbell units are common in carbides, where the C–C bonds (e.g., 1.30 Å in the tetragonal CaC_2 phase) are much shorter than normal C–C single bonds (1.54 Å in diamond and ethane), meaning the bond orders for the C–C bonds in carbides are much greater than 1; usually it is mentioned as a triple bond. In contrast, the Ge–Ge dumbbells in $SrGe_3$ have longer bond distances than those of elemental germanium (diamond structure, 2.45 Å), showing that the bond orders for Ge–Ge dumbbells are less than 1. This observation suggests that extra electrons should be accommodated in the antibonding orbitals of Ge–Ge anionic dumbbells. The detailed electronic structure of $SrGe_3$ is discussed below.

The $SrGe_3$ samples showed a metallic luster, which suggests that the compound is metallic. We performed a magnetic susceptibility measurement using a bulk $SrGe_3$ sample and found that $SrGe_3$ is a superconductor with $T_c = 6.0$ K. The temperature dependence of the magnetic susceptibility at low temperature is shown in Figure 2. The zero-field-cooling and field-cooling curves pass through zero magnetization at 6.0 K and then show a rapid decrease to negative values, exhibiting a superconducting transition. The superconducting volume fraction calculated from the zero-field-cooling plot at 2 K is 91%. This clearly indicates that the transition is because of $SrGe_3$.

The DOS of $SrGe_3$ is shown in Figure 3. We used the measured lattice constants and atomic parameters for all calculations without any optimization. According to the way of contribution of germanium orbitals, there are two parts in the DOS plot below the Fermi level (E_F): the upper part from E_F to -5 eV and the lower part from -5 to -12 eV. The lower and upper parts are mainly composed of Ge 4s and 4p orbitals, respectively, as shown in Figure S2 in the SI. We also show a plot of the partial DOS for each site in Figure 3. The Fermi level is in the upper band. This feature strongly suggests that $SrGe_3$ is not a classic Zintl phase but a metallic compound with

Table 2. Atomic Coordinates and Thermal Displacement Parameters of $SrGe_3$

| atom | site | x | y | z | U_{11} | U_{22} | U_{33} | U_{eq} |
|------|------|------------|------------|------------|-------------|-------------|-------------|-------------|
| Sr1 | 4e | $1/2$ | $1/2$ | 0.32894(4) | 0.01262(17) | 0.01262(17) | 0.0105(2) | 0.01193(13) |
| Sr2 | 4d | $1/2$ | 0 | $3/4$ | 0.01153(17) | 0.01153(17) | 0.0087(2) | 0.01060(12) |
| Ge1 | 8i | $1/2$ | 0.83724(5) | $1/2$ | 0.0111(2) | 0.0106(2) | 0.0109(2) | 0.01085(11) |
| Ge2 | 16m | 0.18272(3) | 0.81728(3) | 0.39453(3) | 0.01837(13) | 0.01837(13) | 0.01425(17) | 0.01699(11) |

The anisotropic atomic displacement factor exponent takes the form $-2\pi^2[h^2a^{*2}U_{11} + \dots + 2hka^*b^*U_{12}]$. $U_{12} = U_{23} = U_{13} = 0$ except for Ge2, where $U_{12} = 0.00184(9)$, $U_{23} = 0.00184(9)$, and $U_{13} = -0.00537(12)$.

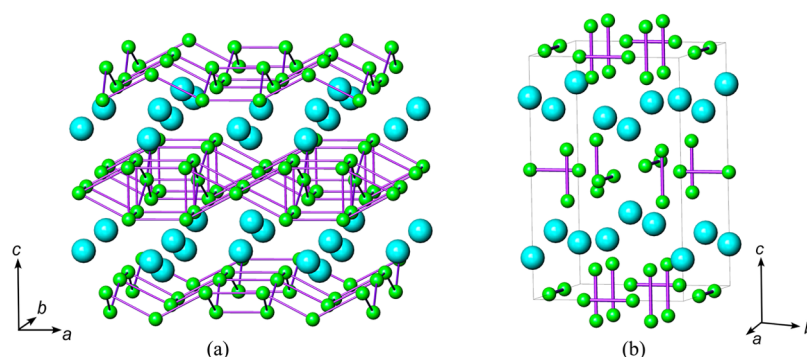


Figure 1. Crystal structure of SrGe_3 . Large blue and small green spheres represent strontium and germanium atoms, respectively. (a) Layer structure composed of strontium ions and germanium layers. (b) Arrangement of the Ge–Ge dumbbells in the unit cell.

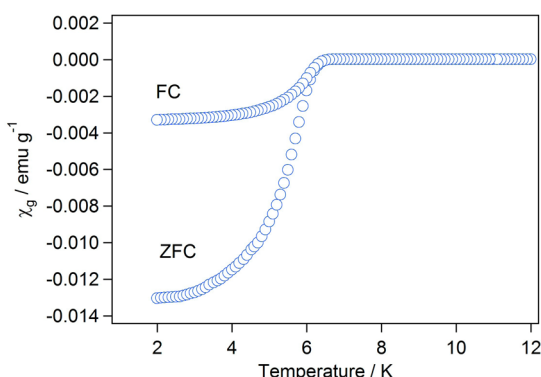


Figure 2. Temperature dependence of the magnetic susceptibility (χ_g) of SrGe_3 .

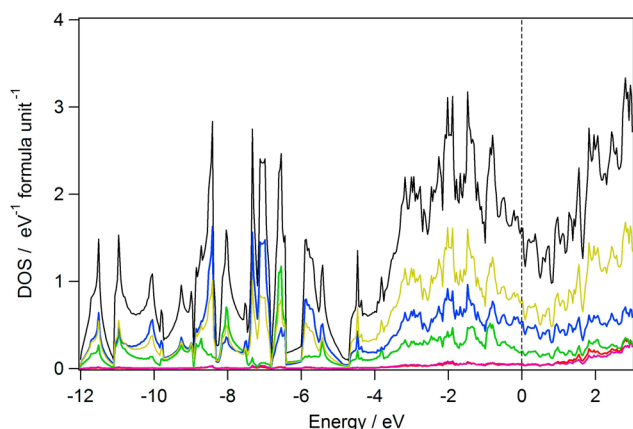


Figure 3. DOS of SrGe_3 . Black, red, purple, green, blue, and yellow lines represent the total, Sr1, Sr2, Ge1, Ge2, and interstitial contributions, respectively.

a covalent substructure of host atoms. We call this type of compound a covalent intermetallic compound.

Figure 4 shows the k dispersions of the SrGe_3 bands along the main symmetry points in reciprocal space. We also calculated the Fermi surfaces, and some of them are shown in Figure 5. Eight bands cross the Fermi level, but five (yellow, orange, pink, purple, and light blue) contribute less to the transport properties because of their small Fermi surfaces. The others (red, blue, and green) have complicated Fermi surfaces. Some of them exhibit relatively three-dimensional features, as shown in Figure 4 (left). There are also cylindrical-shaped surfaces, as shown in the right part of the figure; one is large

and surrounds the X point, and the other is small and surrounds the N point. These bands seem to be highly two-dimensional ones. This probably reflects the crystal structure with a two-dimensional germanium network.

Comparison among Isotypic Compounds. SrGe_3 is isotypic with CaGe_3 and MSi_3 ($M = \text{Ca}, \text{Y}, \text{and Lu}$).^{5,16} The lattice constants of CaGe_3 are $a = 7.6920(4) \text{ \AA}$ and $c = 11.3314(9) \text{ \AA}$, with $V = 670.44(7) \text{ \AA}^3$. The cell volume of SrGe_3 [$729.74(17) \text{ \AA}^3$] is 8.8% larger than that of CaGe_3 because Sr^{2+} is larger than Ca^{2+} : Sr^{2+} ions are about 0.2 \AA larger than Ca^{2+} ions according to the effective ionic radii for 12-coordinated ions. Therefore, strontium trigermanide can form the same structure as calcium trigermanide because the sizes of Sr^{2+} and Ca^{2+} ions are similar.

It is worth noting that the lattice constant a of SrGe_3 [$7.7800(8) \text{ \AA}$] is only 0.088 \AA longer than that of CaGe_3 , while the lattice constant c of SrGe_3 [$12.0561(13) \text{ \AA}$] is much longer (0.7247 \AA) than that of CaGe_3 . Moreover, the Ge–Ge distances in the two independent dumbbells are almost the same or slightly shrink if the guest metal is changed from Ca to Sr (2.549 and 2.599 \AA for CaGe_3 and 2.533 and 2.543 \AA for SrGe_3), while the distances between neighboring dumbbells are almost the same (2.763 and 2.823 \AA for CaGe_3 and 2.781 and 2.843 \AA for SrGe_3).

These observations show that the interconnection of dumbbells is strong enough to form the layered germanium network shown in Figure 1a. When large guest ions are located in the interlayer spaces, the layers accommodate the guest ions by expanding the interlayer spaces without the layers themselves expanding.

Interestingly, the same occurs for yttrium and lutetium trisilicides. The interatomic distances of the dumbbells in CaSi_3 , however, are much shorter than those in the rare-earth trisilicides. We will discuss this later.

The difference of the data sources needs to be considered. One is from Rietveld refinement, and one is from single-crystal analysis, but we consider the interatomic distances of the dumbbells to be slightly shorter in SrGe_3 than in CaGe_3 , even though strontium ions are larger than calcium ions.

This is probably because of the different mixing of Ge 4p and guest-ion orbitals. The Ge–Ge dumbbells accept electrons from the electropositive guest metals, and the number of donated electrons depends on the valence state of the metals. The donated electrons are accommodated in lone pairs of germanium atoms and then in antibonding orbitals after fulfillment of the octet rule. The effective number of donated electrons decreases as the mixing between Ge 4p and guest

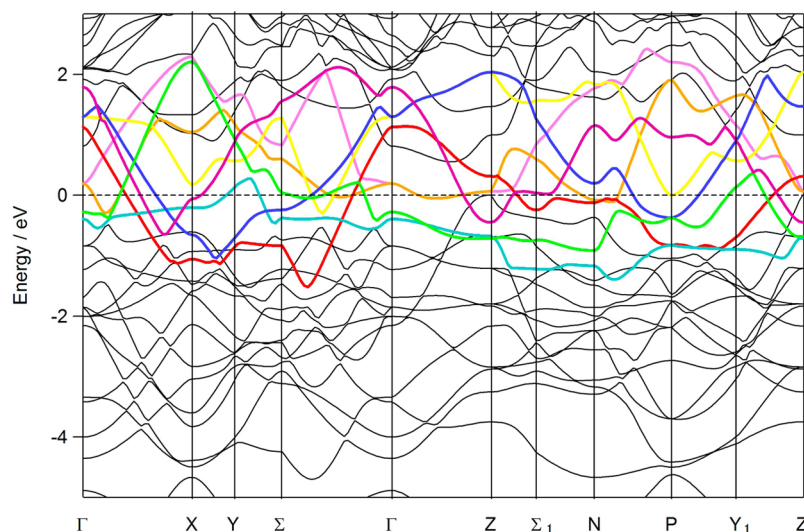


Figure 4. Band structure (k dispersion) of SrGe_3 . Only the conduction bands are colored.

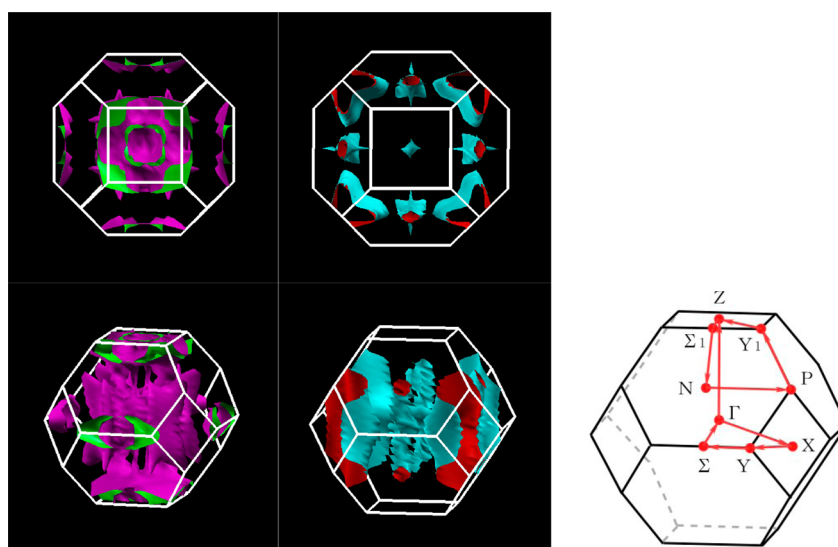


Figure 5. Some Fermi surfaces of SrGe_3 . The left and right surfaces show three- and two-dimensional features, respectively. The Brillouin zone type is BCT_2 .

metal orbitals increases. In other words, the greater the covalency between germanium and the guest ions, the more the dumbbells are reduced.

The mixing between Ge 4p–Sr 5s and/or Ge 4p–Sr 4d orbitals is likely to be more enhanced compared with Ge 4p–Ca 4s and/or Ge 4p–Ca 3d because of the larger 5s and 4d orbitals. Therefore, the dumbbells in SrGe_3 are more reduced than those in CaGe_3 , and the interatomic distances of the dumbbells decrease more because the effective number of electrons donated in the antibonding orbitals of the dumbbells decreases.

This is the reason why the interatomic distances in CaSi_3 are smaller than those in the trivalent metal derivatives. The number of donated electrons is much larger in the latter silicides than in CaSi_3 .

The T_c of SrGe_3 is 0.8 K lower than that of CaGe_3 . This is possibly because of the elongation of the interlayer space between the germanium layers as well as the slight structural changes caused by the electronic condition change of the dumbbell in the germanium layers. The calculated band

structures for strontium and calcium trigermanides are fundamentally the same. The contributions of the two guest sites in the vicinity of E_F are very small.

■ ASSOCIATED CONTENT

📄 Supporting Information

Crystallographic information file (CIF), powder XRD pattern of SrGe_3 (Figure S1), and the partial DOS diagram for each site (Figure S2). The Supporting Information is available free of charge on the ACS Publications website at DOI: 10.1021/acs.inorgchem.5b00989.

■ AUTHOR INFORMATION

Corresponding Author

*E-mail: hfukuoka@hiroshima-u.ac.jp. Phone: +81-82-424-7742.

Notes

The authors declare no competing financial interest.

■ ACKNOWLEDGMENTS

We are grateful to Yasuhiro Shibata and Hayami Ishisako of Hiroshima University for help with the EPMA measurements. This work was supported by a Grant-in-Aid for Scientific Research from the Ministry of Education, Culture, Sports, Science, and Technology of Japan (Grant 24550233).

■ REFERENCES

- (1) Fukuoka, H.; Yamanaka, S. *Phys. Rev. B: Condens. Matter Mater. Phys.* **2003**, *67*, 0945011–0945015.
- (2) Fukuoka, H.; Baba, K.; Yoshikawa, M.; Ohtsu, F.; Yamanaka, S. *J. Solid State Chem.* **2009**, *182*, 2024–2029.
- (3) Fukuoka, H.; Suekuni, K.; Onimaru, T.; Inumaru, K. *Inorg. Chem.* **2011**, *50*, 3901–3906.
- (4) Fukuoka, H.; Tomomitsu, Y.; Inumaru, K. *Inorg. Chem.* **2011**, *50*, 6372–6377.
- (5) Schnelle, W.; Ormeci, A.; Wosylus, A.; Meier, K.; Grin, Y.; Schwarz, U. *Inorg. Chem.* **2012**, *51*, 5509–5511.
- (6) Meier, K.; Cardoso-Gil, R.; Schnelle, W.; Rosner, H.; Burkhardt, U.; Schwarz, U. *Z. Anorg. Allg. Chem.* **2010**, *636*, 1466–1473.
- (7) Aydemir, U.; Akselrud, L.; Carrillo-Cabrera, W.; Candolfi, C.; Oeschler, N.; Baitinger, M.; Steglich, F.; Grin, Y. *J. Am. Chem. Soc.* **2010**, *132*, 10984.
- (8) Castillo, R.; Baranov, A.; Burkhardt, U.; Grin, Y.; Schwarz, U. *Z. Anorg. Allg. Chem.* **2015**, *641*, 355–361.
- (9) Zurek, E.; Yao, Y. *Inorg. Chem.* **2015**, *54*, 2875–2884.
- (10) Castillo, R.; Baranov, A. I.; Burkhardt, U.; Grin, Y.; Schwarz, U. *Z. Anorg. Allg. Chem.* **2015**, *641*, 355.
- (11) Sheldrick, G. *SHELXS-97*; University of Göttingen: Göttingen, Germany, 1997.
- (12) Blaha, P.; Schwarz, K.; Sorantin, P.; Trickey, S. B. *Comput. Phys. Commun.* **1990**, *59*, 399.
- (13) Blaha, P.; Schwarz, K.; Madsen, G. K. H.; Kvasnicka, D.; Luitz, J. *Wien2k, An Augmented Plane Wave + Local Orbitals Program for Calculating Crystal Properties*; Technische Universität Wien: Wien, Austria, 2001.
- (14) Kokalj, A. *Comput. Mater. Sci.* **2003**, *28*, 155.
- (15) Fukuoka, H.; Yamanaka, S.; Matsuoka, E.; Takabatake, T. *Inorg. Chem.* **2005**, *44*, 1460–1465.
- (16) Schwarz, U.; Wosylus, A.; Rosner, H.; Schnelle, W.; Ormeci, A.; Meier, K.; Baranov, K.; Nicklas, M.; Leipe, S.; Müller, C.; Grin, Y. *J. Am. Chem. Soc.* **2012**, *134*, 13558–13561.